Luminescent Diphosphine Dithiolate Complexes of Platinum(II): Synthesis, Characterization, and Structure

Joanne M. Bevilacqua, Juan A. Zuleta, and Richard Eisenberg*

Department of Chemistry, University of Rochester, Rochester, New York 14627

Received June 3, 1993®

The synthesis, characterization, and emission properties of a series of Pt(diphosphine)(dithiolate) complexes are reported. Diphosphine ligands include 1,2-bis(diphenylphosphino)ethane (dppe), 1,2-bis(diphenylphosphino)ethylene (dppv), 1,2-bis(diphenylphosphino)benzene (dppb), 1,2-bis(dicyclohexylphosphino)ethane (chpe), bis(diphenylphosphino)methane (dppm), 1,2-bis(dimethoxyphosphino)ethane (pompom), triphenylphosphine (PPh_3), dimethylphenylphosphine (PMe_2Ph), tricyclohexylphosphine (PCy_3), triphenyl phosphite ($P(OPh)_3$), and triisopropyl phosphite ($P(O\text{-}i\text{-}Pr)_3$). Dithiolate ligands include maleonitriledithiolate (mnt) and 1-(ethoxycarbonyl)-1-cyanoethylene-2,2-dithiolate (ecda). The complexes are readily synthesized by the addition of the diphosphine ligand to Pt(COD)(dithiolate). On the basis of characterizations using NMR and infrared spectroscopies, all of the complexes are assigned square planar coordination geometries with varying degrees of distortion determined by ligand steric and electronic effects. The assignment of square planar coordination is confirmed by single crystal structure determinations of Pt(dppe)(mnt) (**1a**) and Pt(dppb)(mnt) (**3a**). Pink crystals of Pt(dppe)(mnt) (**1a**) ($C_{30}H_{24}N_2P_2PtS_2$) are monoclinic, space group $P2_1/n$ (No. 14), with a = 11.491(4) Å, b = 12.484(2) Å, c = 19.822(7) Å, β = 91.34(1)°, V = 2842.90 Å^3, Z = 4, and final R = 0.029 (R_w = 0.031) for 4793 unique reflections. Orange crystals of Pt(dppb)(mnt) (**3a**) ($C_{34}H_{24}N_2P_2PtS_2$) are monoclinic, space group $P2_1/n$ (No. 14), with a = 10.050(7) Å, b = 19.301(3) Å c, = 15.800(6) Å, β = 94.36(6)°, V = 3056.28 Å^3, Z = 4, and final R = 0.030 (R_w = 0.036) for 5576 unique reflections. The average Pt-S (2.299(7) Å for **1a** and 2.301(2) Å for **3a**) and Pt-P (2.257(2) Å for **1a** and 2.256(7) Å for **3a**) bond distances in each structure agree well with previously reported structural results. The metrical parameters of the mnt chelate ring indicate some degree of metal-ligand delocalization in both structures. The ^{31}P NMR spectra of the phosphines resonances for all of the complexes show platinum satellites ($^1J_{Pt-P}$ = 1100-2500 Hz). In addition, the ecda complexes exhibit complex second-order coupling patterns, arising from the asymmetry of the ecda ligand. All of the complexes exhibit strong emission in the solid state and in frozen glasses at 77 K. Emission spectra are structured for the mnt complexes and broad and featureless for the ecda complexes. Solid-state emission lifetimes at 77 K are in the microsecond range.

Introduction

Luminescent square planar complexes are increasingly studied and well-known. In the past 10 years a large number of reports have appeared describing d^8 complexes of Rh(I), Ir(I), and Pt(II) with chelating diphosphine,[1-4] diolefin,[5] and diimine[6-14] ligands, as well as cyclometalated Pt(II) complexes.[15] In 1983, our laboratory reported the synthesis and characterization of a series of luminescent square planar complexes of general formula $[MLL'(mnt)]^-$ (M = Rh, Ir; L, L' = CO, PR_3, $P(OR)_3$; mnt = maleonitriledithiolate).[16] These complexes exhibited highly structured emission and excitation spectra in the solid state and in frozen solution. From the similarity of the vibronic structure among the Ir and Rh complexes, the shifts in emission maxima as a function of electron donating ability of L and L'; and the observed lifetimes, the emissive transition was assigned as arising from a (d-π^*_{mnt}) excited state.

More recently, we have synthesized a series of Pt(diimine)(dithiolate) complexes (diimine = bipyridine, *o*-phenanthroline, or alkylated derivative; dithiolate = mnt or 1-(ethoxycarbonyl)-1-cyanoethylene-2,2-dithiolate (ecda)).[7-11] It was observed that the absorption spectra of all complexes exhibited solvatochromic behavior, while the emission spectra were dependent upon the dithiolate ligand. Specifically, emission bands from mnt complexes were structured, while ecda analogues possessed essentially featureless emissions. On the basis of emission behavior as a function of temperature for these systems, the mnt complexes were assigned to have a single emitting state, while the ecda complexes showed evidence of multiple emitting states. Different emitting states were thus assigned to the platinum(II) diimine complexes of mnt and ecda with the mnt systems having a (Pt(d)/S(p)-$\pi^*_{dithiolate}$) emissive state, and the ecda complexes possessing a (Pt(d)/S(p)-$\pi^*_{diimine}$) lowest energy excited state. The difference in the emitting states arose from a difference in

® Abstract published in *Advance ACS Abstracts*, December 15, 1993.

(1) Sacksteder, L.; Baralt, E.; DeGraff, B. A.; Lukehart, C. M.; Demas, J. N. *Inorg. Chem.* **1991**, *30*, 2468.
(2) Fordyce, W. A.; Crosby, G. A. *Inorg. Chem.* **1982**, *21*, 1455.
(3) Wan, K.-T.; Che, C.-M. *J. Chem. Soc., Chem. Commun.* **1990**, 140.
(4) Fordyce, W. A.; Rau, H.; Stone, M. L.; Crosby, G. A. *Chem. Phys. Lett.* **1981**, *77*, 405.
(5) Bevilacqua, J. M.; Zuleta, J. A.; Eisenberg, R. *Inorg. Chem.* **1993**, *32*, 3689.
(6) Fordyce, W. A.; Crosby, G. A. *Inorg. Chem.* **1982**, *21*, 1023.
(7) Zuleta, J. A.; Chesta, C. A.; Eisenberg, R. *J. Am. Chem. Soc.* **1989**, *111*, 8916.
(8) Zuleta, J. A.; Burbery, M. S.; Eisenberg, R. *Coord. Chem. Rev.* **1990**, *97*, 47.
(9) Zuleta, J. A.; Bevilacqua, J. M.; Eisenberg, R. *Coord. Chem. Rev.* **1991**, *111*, 237.
(10) Zuleta, J. A.; Bevilacqua, J. M.; Rehm, J. M.; Eisenberg, R. *Inorg. Chem.* **1992**, *31*, 1332.
(11) Zuleta, J. A.; Bevilacqua, J. M.; Proserpio, D. M.; Harvey, P. D.; Eisenberg, R. *Inorg. Chem.* **1992**, *31*, 2396.
(12) Biedermann, J.; Gliemann, G.; Klement, U.; Range, K.-J.; Zabel, M. *Inorg. Chem.* **1990**, *29*, 1884.
(13) Biedermann, J.; Wallfahrer, M.; Gliemann, G. *J. Lumin.* **1987**, *37*, 323.
(14) Chan, C.-W.; Che, C.-M.; Cheng, M.-C.; Wang, Y. *Inorg. Chem.* **1992**, *31*, 4874.
(15) Maestri, M.; Balzani, V.; Deuschel-Cornioley, C.; von Zelewsky, A. *Advances in Photochemistry*; Volman, D., Hammond, G., Neckers, D., Eds.; John Wiley and Sons: New York, 1992; Vol. 17 and references therein.
(16) Johnson, C. E.; Eisenberg, R.; Evans, T. R.; Burberry, M. S. *J. Am. Chem. Soc.* **1983**, *105*, 1795.

0020-1669/94/1333-0258$04.50/0

the $\pi^*_{dithiolate}$ energies for mnt and ecda relative to the lowest unoccupied π^* levels of the diimine.[11]

Platinum complexes containing phosphine and thiolate ligands have been known for some time.[17-22] However, in most of the studies of these systems, the focus has been on their reaction chemistry and not on their electronic structure. Early reports that described monomeric platinum species containing monodentate phosphine and thiolate ligands dealt with their cis–trans isomerization reactions.[21] The compounds were found to be unstable with respect to dimerization and polymerization, yielding mixtures of thiolato bridged oligomers.[17,20] In contrast, complexes containing a bidentate dithiolate ligand and diphosphine or two monodentate phosphine donor ligands did not exhibit a tendency to dimerize or polymerize.

To probe further the electronic structure of emissive Pt complexes, we have undertaken a more extensive characterization of complexes of the type PtL_2(dithiolate) in which L are phosphines and phosphites. The present study describes the synthesis and characterization of these systems as well as the single-crystal X-ray structure determination of two of these complexes. In accord with the absence of a low-lying $\pi^*_{diimine}$ level, none of the complexes exhibits the solvatochromic behavior or the room-temperature solution emission of the Pt(diimine)(dithiolate) complexes. However, all of the complexes are luminescent at 77 K, and, as with the diimine analogues, significant differences in the emission spectra exist between the mnt and ecda complexes.

Experimental Section

Materials and Methods. The reagents K_2PtCl_4 (Johnson-Matthey); 1,2-bis(diphenylphosphino)ethane (dppe), triphenylphosphine (PPh_3), triphenyl phosphite ($P(OPh)_3$), and triisopropyl phosphite ($P(O\text{-}i\text{-}Pr)_3$) (Aldrich); 1,2-bis(diphenylphosphino)ethylene (dppv), 1,2-bis(diphenylphosphino)benzene (dppb), 1,2-bis(dicyclohexylphosphino)ethane (chpe), bis(diphenylphosphino)methane (dppm), dimethylphenylphosphine (PMe_2Ph), and tricyclohexylphosphine (PCy_3) (Strem) were used as received without further purification. The ligand 1,2-bis(dimethoxyphosphino)ethane (pompom) was provided by Dr. William D. Jones. Na_2(mnt),[23] K_2(ecda),[24] $Pt(NCPh)_2Cl_2$,[25] Pt(COD)(mnt), and Pt(COD)(ecda) (where COD = 1,5-cyclooctadiene, mnt = maleonitriledithiolate, and ecda = 1-(ethoxycarbonyl)-1-cyanoethylene-2,2-dithiolate),[5,16] were prepared according to literature procedures. Syntheses were performed under N_2 using standard Schlenk and inert atmosphere techniques. Reactions were carried out at room temperature. Solvents were of spectral grade quality, and were dried, distilled, and rigorously degassed before use.

General Method. Complexes (**1a,b-11a,b**) were made according to Scheme 1. A typical reaction began with 0.125 g of Pt(COD)(dithiolate) (0.28 mmol of Pt(COD)(mnt) or 0.26 mmol of Pt(COD)(ecda)) dissolved in acetone. To this was added 1.1 or 2.2 equiv of the respective diphosphine or phosphine ligand dissolved in acetone. After 1–6 h, the solvent volume was reduced to ~5 mL, and then 20 mL of ether was added. The resulting precipitate was collected by centrifugation, then washed with ethanol and ether, and dried under vacuum.

Alternative Method. Some compounds were also made by an alternative method in which the Pt(diphosphine)Cl_2 complex was first prepared. A typical reaction began with 0.150 g of $Pt(NCPh)_2Cl_2$ dissolved in acetone. To this was added 1.3–2.5 equiv of the phosphine ligand dissolved in acetone. After 6 h, the resulting white Pt(diphosphine)Cl_2 product was collected. This precursor was then reacted with 1.5 equiv of the desired dithiolate dissolved in methanol for 3 h. Reduction of the solvent volume to ~5 mL and addition of 20 mL of ether caused the product to precipitate. Workup of the product was performed as in the general method.

Scheme 1

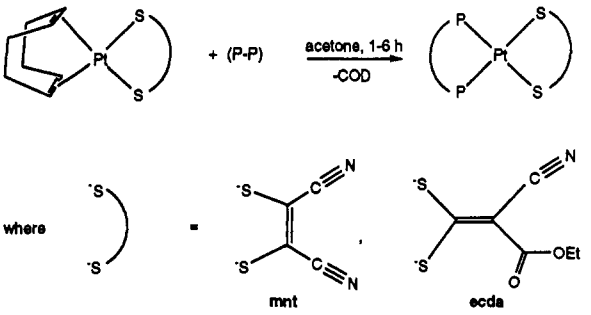

	(P-P)	(S-S)
1a	dppe	mnt
2a	dppv	mnt
3a	dppb	mnt
4a	chpe	mnt
7a	PPh_3	mnt
8a	PMe_2Ph	mnt
1b	dppe	ecda
2b	dppv	ecda
3b	dppb	ecda
4b	chpe	ecda
5b	dppm	ecda
6b	pompom	ecda
7b	PPh_3	ecda
8b	PMe_2Ph	ecda
9b	PCy_3	ecda
10b	$P(OPh)_3$	ecda
11b	$P(O\text{-}i\text{Pr})_3$	ecda

Pt(dppe)(mnt) (1a). Both methods described yielded the same pale yellow product. IR (KBr, cm^{-1}): 3055 (C—H), 2203 (CN), 1435 (C=C), 1152 (C—S), 1103 (C—P).

Pt(dppv)(mnt) (2a). Both methods described yielded the same tan product. IR (KBr, cm^{-1}): 3009 (C—H), 2205 (CN), 1435 (C=C), 1154 (C—S), 1103 (C—P). Anal. Calcd for $PtC_{30}H_{22}N_2P_2S_2$: C, 49.24; H, 3.03. Found: C, 49.04; H, 2.98.

Pt(dppb)(mnt) (3a). IR (KBr, cm^{-1}) of the off-white powder: 3057 (C—H), 2209 (CN), 1433 (C=C), 1150 (C—S), 1101 (C—P).

Pt(chpe)(mnt) (4a). IR (KBr, cm^{-1}) of the pink powder: 2928 (C—H), 2199 (CN), 1447 (C=C), 1162 (C—S), 1113 (C—P). Anal. Calcd for $PtC_{30}H_{48}N_2P_2S_2$: C, 47.54; H, 6.38. Found: C, 47.27; H, 6.26.

Pt(PPh_3)$_2$(mnt) (7a). IR (KBr, cm^{-1}) of the golden-colored product: 2200 (CN), 1432 (C=C), 1146 (C—S), 1103 (C—P).

Pt(PMe_2Ph)$_2$(mnt) (8a). IR (KBr, cm^{-1}) of the pink powder: 3008 (C—H), 2160 (CN), 1425 (C=C), 1138 (C—S), and 1082 (br, C—P).

Pt(dppe)(ecda) (1b). Both methods described yielded the same off-white product. IR (KBr, cm^{-1}): 3054 (C—H), 2205 (CN), 1699 (C=O), 1458 (C=C), 1144 (C—S); 1103 (C—P). Anal. Calcd for $PtC_{32}H_{30}O_2NP_2S_2$: C, 49.23; H, 3.74. Found: C, 48.82; H, 3.84.

Pt(dppv)(ecda) (2b). IR (KBr, cm^{-1}) of the off-white product: 2942 (C—H), 2208 (CN), 1712 (C=C), 1137 (C—S), and 1101 (C—P). Anal. Calcd for $PtC_{32}H_{28}NO_2P_2S_2$: C, 49.35; H, 3.49; P, 7.95. Found: C, 49.07; H, 3.50; P, 7.67.

Pt(dppb)(ecda) (3b). Both methods described yielded the same off-white product. IR (KBr, cm^{-1}): 3055 (C—H), 2205 (CN), 1692 (C=O), 1435 (C=C), 1140 (C—S), 1108 (C—P).

Pt(chpe)(ecda) (4b). IR (KBr, cm^{-1}) of the slightly pink powder: 2924 (C—H), 2202 (CN), 1689 (C=O), 1446 (C=C), 1168 (C=S), 1105 (C—P).

Pt(dppm)(ecda) (5b). A solution of 0.09 g of bis(diphenylphosphino)-methane (0.24 mmol) dissolved in 20 mL of acetone was added to 0.11 g (0.22 mmol) of Pt(COD)(ecda) dissolved in 30 mL of acetone. The solution became colorless within 3 h. The solvent was evaporated to ~5 mL. Addition of 10 mL of ether resulted in a yellow oil. After three rapid additions of 2 mL of acetone and 10 mL of ethanol, a cream-colored precipitate was recovered which was collected by centrifugation and then washed with ethanol and ether. IR (KBr, cm^{-1}): 3055 (C—H), 2203

(17) Braterman, P. S.; Wilson, V. A.; Joshi, K. K. *J. Organomet. Chem.* **1971**, *31*, 123.
(18) Zanella, R.; Ros, R.; Graziani, M. *Inorg. Chem.* **1973**, *12*, 2736.
(19) Rauchfuss, T. B.; Roundhill, D. M. *J. Am. Chem. Soc.* **1975**, *97*, 3386.
(20) Rauchfuss, T. B.; Shu, J. S.; Roundhill, D. M. *Inorg. Chem.* **1976**, *15*, 2096.
(21) Lai, R. D.; Shaver, A. *Inorg. Chem.* **1981**, *20*, 477.
(22) Fazlur-Rahman, A. K.; Verkade, J. G. *Inorg. Chem.* **1992**, *31*, 5331.
(23) Davidson, A.; Holm, R. H. *Inorg. Synth.* **1967**, *10*, 8.
(24) Jensen, K. A.; Henriksen, L. *Acta Chem. Scand.* **1968**, *22*, 1108.
(25) Anderson, G. K.; Lin, M. *Inorg. Synth.* **1989**, *26*, 345.

(CN), 1627 (C=O), 1454 (C=C), 1168 (C—S), 1101 (C—P). Anal. Calcd for $PtC_{31}H_{27}NO_2P_2S_2$: C, 48.56; H, 3.55. Found: C, 47.82; H, 3.47.

Pt(pompom)(ecda) (6b). IR (KBr, cm^{-1}) of the pale yellow precipitate: 2969 (C—H), 2205 (CN), 1690 (C=O), 1458 (C=C), 1152 (C—S), and 1103 (C—P).

$Pt(PPh_3)_2$(ecda) (7b). Both methods described yielded the same yellow product. IR (KBr, cm^{-1}): 3055 (C—H), 2205 (CN), 1692 (C=O), 1435 (C=C), 1146 (C—S), and 1096 (C—P).

$Pt(PMe_2Ph)_2$(ecda) (8b). IR (KBr, cm^{-1}) of the pale yellow precipitate: 2976 (C—H), 2203 (CN), 1688 (C=O), 1449 (C=C), 1167 (C—S), and 1107 (C—P).

$Pt(PCy_3)_2$(ecda) (9b). IR (KBr, cm^{-1}) of the yellow powder: 2928 (C—H), 2226 (CN), 1690 (C=O), 1444 (C=C), 1144 (C—S), 1103 (sh, C—P).

$Pt(P(OPh)_3)_2$(ecda) (10b). IR (KBr, cm^{-1}) of the pale yellow powder: 3050 (C—H), 2222 (CN), 1688 (C=O), 1440 (C=C), 1147 (C—S), 1105 (C—P).

$Pt(P(O\text{-}iPr)_3)_2$(ecda) (11b). IR (KBr, cm^{-1}) of the off-white powder: 2980 (C—H), 2207 (CN), 1697 (C=O), 1460 (C=C), 1142 (C—S), 1101 (C—P).

Spectroscopic Characterization. ^1H (400 MHz), ^{13}C (100.62 MHz), and ^{31}P (161.97 MHz) NMR spectra were recorded on a Bruker AMX-400 spectrometer. Chemical shifts are reported downfield from internal solvent peaks; acetone-d_6 (δ_H = 2.04) and chloroform-d_1 (δ_H = 7.24) for ^1H and DMSO-d_6 (δ_C = 39.5) for ^{13}C. H_3PO_4 (δ_P = 0) was used as an external standard for ^{31}P. Microanalyses were performed by Galbraith Laboratories, Ltd. Infrared spectra were obtained from KBr pellets on a Mattson Sirius 100 FTIR spectrophotometer. Absorption spectra were recorded on a Hewlett-Packard HP-8452A diode-array UV–visible spectrophotometer. Low-temperature emission and excitation measurements were performed on a Spex Fluorolog fluorescence spectrophotometer using a liquid-nitrogen dewar equipped with quartz windows. The emission spectra were recorded with 370-nm excitation, and a collection wavelength of 580 nm was used to record the excitation spectra. Low-temperature lifetimes were measured by transient digitization, and the instrumental setup has been described elsewhere.[5] Low-temperature emission spectra were recorded in DMM glasses (DMF/CH_2Cl_2/MeOH in 1:1:1 v/v/v) or in a KBr matrix.

Structure Determinations. Single-crystal X-ray structure determinations were carried out using an Enraf-Nonius CAD4 diffractometer with Mo Kα radiation (λ = 0.710 73 Å) for data collection. Texsan software was used for data reduction, structure solution, and least-squares refinement.

Crystal Structure Determination of Pt(dppe)(mnt) (1a). A pink prismatic crystal of Pt(dppe)(mnt) (**1a**) (dimensions 0.45 × 0.11 × 0.038 mm^3) was grown from a room-temperature chloroform solution. The crystals were found to be air stable at room temperature. Crystal, data collection, and refinement parameters are summarized in Table 1. The monoclinic space group $P2_1/n$ was uniquely determined with the bis chelate complex in general positions of the space group; successful refinement of the structure confirmed the space group assignment. Heavy-atom methods were used to locate the platinum and two sulfur atoms, while subsequent cycles of least-squares refinements and difference Fourier maps were used to located the remaining non-hydrogen atoms. Hydrogen atoms were placed at calculated positions around the 1,2-bis(diphenylphosphino)ethane ligand.

Crystal Structure Determination of Pt(dppb)(mnt) (3a). A crystal suitable for X-ray diffraction analysis was grown by slow evaporation of a solution of the complex in chloroform. The crystals were found to be air stable at room temperature. An orange prism (dimensions 0.30 × 0.34 × 0.41 mm^3) was mounted on a glass fiber. Crystal, data collection, and refinement parameters are summarized in Table 1. The monoclinic space group $P2_1/n$ was uniquely determined with the bis chelate complex in general positions of the space group; successful refinement of the structure confirmed the space group assignment. Heavy-atom methods were employed to locate the platinum and two sulfur atoms. Remaining atoms were located using cycles of Fourier maps and least squares refinements. In the last refinement all non-hydrogen atoms were described with anisotropic thermal parameters. Hydrogen atoms were placed at calculated positions around the 1,2-bis(diphenylphosphino)benzene ligand.

Results and Discussion

As shown in Scheme 1, all of the Pt complexes described here are readily prepared by reaction of Pt(COD)(mnt)[16] and Pt(COD)(ecda)[5] with a slight excess of phosphine ligand, 1.1 equiv for bidentate diphosphine chelating agents and 2.2 equiv for the monodentate ligands. An alternative method of synthesis in which the dithiolate is added to Pt(diphosphine)Cl_2 was also successful and is described in the Experimental Section. This method, however, involves more steps and leads to lower product yield. All complexes were isolated in high yields (85–95%) as off-white, pink, or bright yellow powders. The complexes are soluble in most organic solvents but insoluble in ether, alcohol, and hexane. Complexes were characterized by electronic, infrared, and ^1H, ^{13}C, and ^{31}P NMR spectroscopies and, in two cases, by X-ray crystallography. Also, elemental analyses were performed on selected complexes. All complexes are air-stable for weeks in the solid state, although in solution their stability decreased to days. The solution stability of the complexes to decomposition in air depends on the nature of the phosphine ligand in the order bidentate diphosphine with aromatic substituents (most stable) > bidentate diphosphine with aliphatic substituents > monodentate phosphine with aromatic substituents > bidentate diphosphine with alkoxy substituents > monodentate phosphine with alkoxy substituents > monodentate phosphine with aliphatic substituents (least stable). Also, the mnt complexes are more stable than the ecda analogues.

^1H and ^{13}C NMR data for all of the complexes are given in Table 2 with appropriate assignments. The mnt complexes (**1a–8a**) exhibit a single resonance in each $^{31}P\{^1H\}$ NMR spectrum with a pair of ^{195}Pt satellites (Table 2). The magnitude of J_{Pt-P} is consistent with a square planar coordination geometry having two equivalent cis phosphine donors.[26,27] This observation is supported by the work of Fazlur-Rahman and Verkade[22] on analogous symmetrical dithiolate Pt(P–P)(S–S) complexes. As has been observed previously for analogous Pt(II) phosphine complexes, the chemical shifts of the ^{31}P resonances are dependent on the size of the chelate ring.[22,28–31] The phosphine donors in

Table 1. Crystallographic Data for Pt(P–P)(S–S)[a]

	Pt(dppe)(mnt) (**1a**)	Pt(dppb)(mnt) (**3a**)
chem formula	$C_{30}H_{24}N_2P_2PtS_2$	$C_{34}H_{24}N_2P_2PtS_2$
fw	733.69	781.73
lattice type	monoclinic	monoclinic
space group	$P2_1/n$ (No. 14)	$P2_1/n$ (No. 14)
Z	4	4
a, Å	11.491(4)	10.050(7)
b, Å	12.484(2)	19.301(3)
c, Å	19.822(7)	15.800(6)
α, deg	90	90
β, deg	91.34(1)	94.36(6)
γ, deg	90	90
V, Å^3	2842.90	3056.28
ρ_{calc}, g/cm^3	1.714	1.699
T, °C	25	25
μ, cm^{-1}	52.6	48.9
$\lambda_{Mo\ K\alpha}$ (graphite monochromated radiation), Å	0.710 69	0.710 69
R	0.0287	0.0302
R_w	0.0306	0.0360

[a] $R = \{\sum||F_o| - |F_c||\}/\{\sum|F_o|\}$; $R_w = [\sum w(|F_o| - |F_c|)^2]^{1/2}/\{\sum wF_o^2\}$, where $w = [\sigma^2(F_o) + (\rho F_o^2)^2]^{1/2}$ for the non-Poisson contribution weighting scheme. The quantity minimized was $\sum w(|F_o| - |F_c|)^2$. Source of scattering factors f_o, f', f'': Cromer, D. T.; Waber, J. T. *International Tables for X-Ray Crystallography*; Kynoch Press: Birmingham, England, 1974; Vol. IV, Tables 2.2B and 2.3.1.

(26) Pregosin, P. S.; Kunz, R. W. *NMR Basic Principles and Progress*; Diehl, P.; Fluck, E., Kosfeld, R., Eds.; Springer-Verlag: Berlin, 1979; Vol. 16.
(27) *Phosphorous-31 NMR Spectroscopy in Stereochemical Analysis*; Verkade, J. G., Quin, L. D., Eds.; VCH Publishers, Inc.: New York, 1986; Vol. 8.
(28) Lindner, E.; Fawzi, R.; Mayer, H. A.; Eichele, K.; Hiller, W. *Organometallics* **1992**, *11*, 1033.
(29) Hietkamp, S.; Stuffken, D. J.; Vrieze, K. *J. Organomet. Chem.* **1979**, *169*, 107.
(30) Appleton, T. G.; Bennett, M. A.; Tomkins, I. B. *J. Chem. Soc., Dalton Trans.* **1976**, 439.

Table 2. ^{1}H, ^{13}C, and ^{31}P NMR Data for Complexes **1–11**[a]

sample	^{1}H NMR	^{13}C NMR	$^{31}P\{^{1}H\}$ NMR
1a	7.7–7.6 (m, 8H) C_6H_5 7.6–7.4 (m, 12H) C_6H_5 2.55 (complex multiplet, 4H) CH_2CH_2		45.63 (s, $^{1}J_{Pt-P}$ = 1397 Hz)
2a	7.7–7.2 (m, 22H)		54.89 (s, $^{1}J_{Pt-P}$ = 1401 Hz)
3a	7.7–7.3 (m, 24H)		44.62 (s, $^{1}J_{Pt-P}$ = 1391 Hz)
4a	2.1–1.2 (m, 48H)		68.02 (s, $^{1}J_{Pt-P}$ = 1361 Hz)
7a	7.5–7.1 (m, 30H)		16.73 (s, $^{1}J_{Pt-P}$ = 1456 Hz)
8a	7.5–7.3 (m, 10H) 1.72 (m, 12H)		−18.85 (s, $^{1}J_{Pt-P}$ = 1381 Hz)
1b	7.7–7.6 (m, 8H) C_6H_5 7.5–7.4 (m, 12H) C_6H_5 4.16 (q, 2H, J_{H-H} = 10.3 Hz) OCH_2CH_3 2.37 (complex multiplet, 4H) CH_2CH_2 1.26 (t, 3H, J_{H-H} = 6.8 Hz) OCH_2CH_3		41.55 (d, $^{1}J_{Pt-P}$ = 1517 Hz, $^{2}J_{P-P}$ = 10.7 Hz) 40.66 (d, $^{1}J_{Pt-P}$ = 1448 Hz, $^{2}J_{P-P}$ = 10.7 Hz)
2b[b]	7.95 (complex multiplet, 2H) HC=CH 7.8–7.7 (m, 8H) C_6H_5 7.6–7.5 (m, 12H), C_6H_5 4.11 (q, 2H, J_{H-H} = 9.1 Hz) OCH_2CH_3 1.23 (t, 3H, J_{H-H} = 9.1 Hz) OCH_2CH_3	204.6 (s) CN 161.7 (s) COOEt 145.8 (m) HC=CH 132.5 (t) C_6H_5 129.4 (m) C_6H_5 114.6 (s) S_2C=C 98.0 (s) S_2C=C 60.0 (s) OCH_2CH_3 13.8 (s) OCH_2CH_3	54.55 (d, $^{1}J_{Pt-P}$ = 1513 Hz, $^{2}J_{P-P}$ = 5.6 Hz) 53.91 (d, $^{1}J_{Pt-P}$ = 1441 Hz, $^{2}J_{P-P}$ = 5.6 Hz)
3b[b]	8.0–7.5 (m, 24H) 4.08 (q, 2H, J_{H-H} = 7.1 Hz) OCH_2CH_3 1.18 (t, 3H, J_{H-H} = 7.0 Hz) OCH_2CH_3		40.16 (d, $^{1}J_{Pt-P}$ = 1506 Hz, $^{2}J_{P-P}$ = 10.3 Hz) 39.74 (d, $^{1}J_{Pt-P}$ = 1430 Hz, $^{2}J_{P-P}$ = 10.3 Hz)
4b	4.19 (q, 2H, J_{H-H} = 7.2 Hz) OCH_2CH_3 2.1–1.2 (m, 51H)		64.11 (d, $^{1}J_{Pt-P}$ = 1491 Hz, $^{2}J_{P-P}$ = 3.2 Hz) 63.47 (d, $^{1}J_{Pt-P}$ = 1426 Hz, $^{2}J_{P-P}$ = 3.2 Hz)
5b[b]	8.0–7.8 (m, 8H) C_6H_5 7.6–7.4 (m, 12H) C_6H_5 5.25 (t, 2H, J_{H-H} = 10.8 Hz) P_2CH_2 4.13 (q, 2H, J_{H-H} = 7.2 Hz) OCH_2CH_3 1.25 (t, 3H, J_{H-H} = 6.8 Hz) OCH_2CH_3		7.63 (d, $^{1}J_{Pt-P}$ = 1321 Hz, $^{2}J_{P-P}$ = 70.4 Hz) 6.36 (d, $^{1}J_{Pt-P}$ = 1192 Hz, $^{2}J_{P-P}$ = 70.4 Hz)
6b[b]	4.13 (q, 2H, J_{H-H} = 10.3 Hz) OCH_2CH_3 3.86 (s, 6H) OCH_3 3.84 (s, 6H) OCH_3 2.1 (complex multiplet, 4H) CH_2CH_2 1.20 (t, 3H, J_{H-H} = 6.8 Hz) OCH_2CH_3		163.8 (s, $^{1}J_{Pt-P}$ = 1925 Hz) 162.7 (s, $^{1}J_{Pt-P}$ = 2020 Hz)
7b	7.5–7.1 (m, 30H) C_6H_5 4.09 (q, 2H, J_{H-H} = 10.3 Hz) OCH_2CH_3 1.19 (t, 3H, J_{H-H} = 6.8 Hz) OCH_2CH_3		19.04 (d, $^{1}J_{Pt-P}$ = 1577 Hz, $^{2}J_{P-P}$ = 22.1 Hz) 18.35 (d, $^{1}J_{Pt-P}$ = 1500 Hz, $^{2}J_{P-P}$ = 22.1 Hz)
8b	7.5–7.2 (m, 10H) C_6H_5 4.22 (q, 2H, J_{H-H} = 7.6 Hz) OCH_2CH_3 1.51 (m, 12H) CH_3 1.30 (t, 3H, J_{H-H} = 8.6 Hz) OCH_2CH_3		−18.22 (d, $^{1}J_{Pt-P}$ = 1514 Hz, $^{2}J_{P-P}$ = 24.5 Hz) −18.67 (d, $^{1}J_{Pt-P}$ = 1445 Hz, $^{2}J_{P-P}$ = 24.5 Hz)
10b[b]	7.4–7.1 (m, 30H) OC_6H_5 4.06 (q, 2H, J_{H-H} = 7.1 Hz) OCH_2CH_3 1.19 (t, 3H, J_{H-H} = 7.0 Hz) OCH_2CH_3		84.68 (d, $^{1}J_{Pt-P}$ = 2240 Hz, $^{2}J_{P-P}$ = 20.3 Hz) 83.57 (d, $^{1}J_{Pt-P}$ = 2110 Hz, $^{2}J_{P-P}$ = 20.3 Hz)
11b[b]	4.83 (m, 6H) $OCH(CH_3)_2$ 4.19 (q, 2H, J_{H-H} = 7.7 Hz) OCH_2CH_3 1.35 (m, 36H) $OCH(CH_3)_2$ 1.27 (t, 3H, J_{H-H} = 8.4 Hz) OCH_2CH_3		83.93 (d, $^{1}J_{Pt-P}$ = 2478 Hz, $^{2}J_{P-P}$ = 23.4 Hz) 82.96 (d, $^{1}J_{Pt-P}$ = 2349 Hz, $^{2}J_{P-P}$ = 23.4 Hz)

[a] Chemical shift values are reported in ppm. All ^{1}H and ^{31}P NMR spectra were taken in chloroform-*d* except where noted. The ^{13}C NMR spectrum was recorded in DMSO-d_6. [b] Recorded in acetone-d_6.

five-membered chelate rings (complexes **1a,b–4a,b**) are less shielded than those in four-membered chelate rings (complex **5b**), the ranges being 68–39 and 7-6 ppm, respectively. The chemical shifts of the ^{31}P resonances are less sensitive to dithiolate chelate ring size. As shown in Table 2 for a given PtL_2 moiety where L_2 is a diphosphine or two monodentate phosphines, the ^{31}P chemical shift changes very little (~4 ppm) upon going from mnt to ecda.

Complexes **1b–11b** have $^{31}P\{^{1}H\}$ NMR spectra that are more complicated because ecda is an unsymmetrical dithiolate (Scheme 1), which causes the *cis* phosphines attached to platinum to be inequivalent (an AB spin system). This inequivalence leads to slightly different coupling constants J_{Pt-P} (^{195}Pt, $I = {}^{1}/_{2}$, 33.8% natural abundance) which in turn result in platinum satellites exhibiting different degrees of second order behavior, as illustrated in Figure 1. The large central resonances in the $^{31}P\{^{1}H\}$ NMR spectra of Figure 1 show characteristic AB patterns for Pt(dppv)(ecda) (**2b**) (δ = 54.55 and 53.91 ppm) and $Pt(PMe_2Ph)_2$(ecda) (**8b**) (δ = −18.22 and −18.67 ppm). The resonances, especially that of **8b**, possess some second-order character because the chemical shift difference in each, $\Delta\delta_{P-P}$, in Hz (*ie.*, $\nu_{P1}-\nu_{P2}$), is close in frequency to the phosphorus-phosphorus coupling constant, J_{P-P}. For complex **2b**, $\Delta\delta$ in Hz is 103.6 Hz while J_{P-P} is 5.6 Hz whereas for **8b**, $\Delta\delta$ is 72.9 Hz and J_{P-P} is 24.5 Hz. For the platinum satellites, the extent of second-order behavior changes as a consequence of the different platinum–phosphorus coupling constants, J_{Pt-P}, of the two ^{31}P resonances in addition to their different chemical shifts. The downfield satellites of P_1 and P_2 (63.89 and 62.80 ppm for **2b** and −8.87 and −9.75 ppm for **8b**) move further away from each other so that the chemical shift differences (176.6 Hz for **2b**, and 142.6 Hz for **8b**) become much larger than J_{P-P} (5.6 and 24.5 Hz, respectively). For both **2b** and **8b**, the downfield components appear as an essentially first-order pair of doublets as in Figure 1. The opposite is true for the upfield satellites of P_1 and P_2 (45.21 and 45.01 ppm for **2b**, and

(31) Merriwether, K. S.; Leto, J. R. *J. Am. Chem. Soc.* **1961**, *83*, 3182.

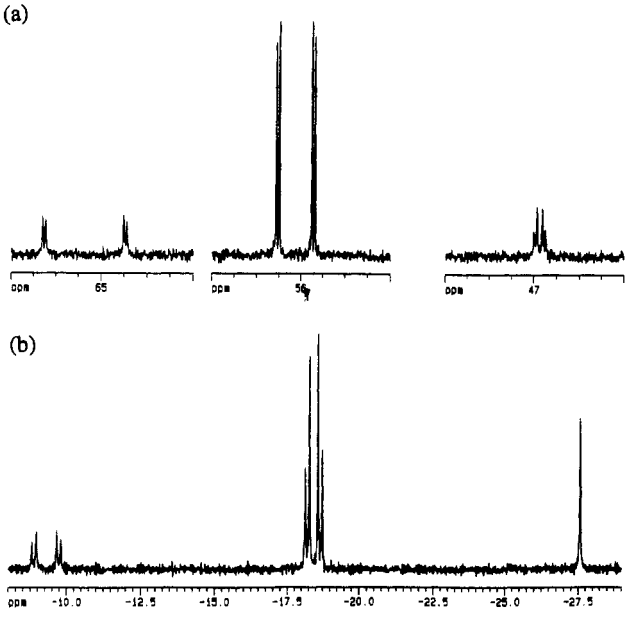

Figure 1. $^{31}P\{^1H\}$ NMR spectrum of (a) Pt(dppv)(ecda) (**2b**) and (b) $Pt(PMe_2Ph)_2$(ecda) demonstrating the effect of the unsymmetrical dithiolate, ecda. The central resonance is due to the AB subset of the ABX spin system. The high- and low-field resonances show the effect of ^{195}Pt on the inequivalent phosphine resonances.

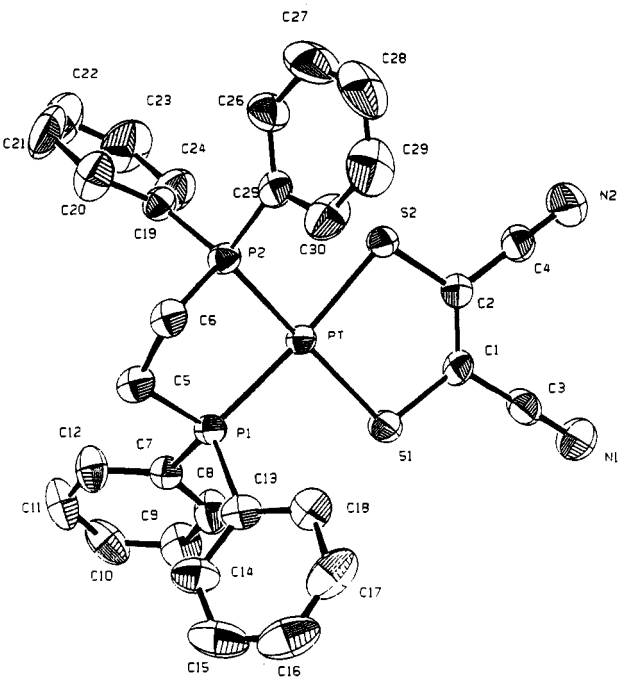

Figure 2. Molecular structure and atom numbering of the non-hydrogen atoms (ORTEP diagram, 50% thermal ellipsoids) of Pt(dppe)(mnt) (**1a**).

-27.57 and -27.58 ppm for **8b**) which move closer together. Here the chemical shift difference (32.4 Hz for **2b**, and 1.6 Hz for **8b**) is on the order of J_{P-P} (5.6 and 24.5 Hz, respectively).[32,33] For $Pt(PMe_2Ph)_2$(ecda) (**8b**), the upfield components are so close together that they become a slightly broadened singlet due to the apparent equivalence of the two ^{195}Pt-split phosphorus components.

The square planar geometry about the platinum was confirmed by single crystal X-ray diffraction studies. ORTEP diagrams of Pt(dppe)(mnt) (**1a**) and Pt(dppb)(mnt) (**3a**) are shown as Figures 2 and 3, respectively. Selected bond distances and angles for both structures are presented in Table 3. Supplementary material contains the final anisotropic thermal parameters, calculated hydrogen positional parameters, a complete tabulation of bond distances and angles, and a listing of observed and calculated structure factor amplitudes.

The Pt–P (2.262(2) and 2.252(2) Å for **1a** and 2.247(2) and 2.266(3) Å for **3a**) and Pt–S (2.303(2) and 2.296(2) Å for **1a** and 2.309(3) and 2.293(2) Å for **3a**) bond lengths are comparable to bond distances in similar complexes that have *trans* phosphorus and sulfur ligands. Typical Pt–P and Pt–S bond distances for complexes of the type PtLL'(S–S) (L, L' = PPh_3, Cl, C(O)Me; S–S = CS_2, dithiocarbamate, dithiolate) are in the ranges 2.24–2.28 and 2.29–2.35 Å, respectively.[34-37] The geometry of the mnt moiety in **1a** and **3a** indicates some delocalization within the chelate ring with metrical parameters similar to other structures containing mnt ligands.[5,38-43] The S–C bond lengths (1.727(7) and 1.737(7) Å for **1a** and 1.731(7) and 1.720(7) Å for **3a**) are in the range of those for other metal–mnt complexes (1.70–1.75 Å) where M = Ni(II), Pt(II), Co(II), and Cu(I) indicating that the S–C bond length is independent of coordinated metal and metal oxidation state. The C1–C2 bond length (1.34(1) and 1.38(1) Å for **1a** and **3a**, respectively) is typical of a C=C double bond, while the C1–C3 and C2–C4 bond lengths (1.43(1) and 1.42(1) Å, respectively, for **1a** and 1.43(1) and 1.44(1) Å, respectively, for **3a**) are shorter than localized single C–C bonds supporting the conclusion of delocalization over the π-electron system of the mnt ligand.

The major difference between **1a** and **3a** lies in the diphosphine chelate ring. In **1a** there is a longer C5–C6 bond distance than in **3a** (1.54(1) versus 1.393(8) Å, respectively). The shorter C–C bond in **3a** is a manifestation of the carbon backbone of the diphosphine chelate of **3a** which is an aromatic *o*-phenylene group. As shown in Figure 3b, there is a 12.02° angle between the plane formed by P1–P2–Pt–S1–S2 and that containing P1–C5–C6–C7–C8–C9–C10–P2.

Electronic Absorption Spectroscopy. All complexes have a broad, intense absorption band between 340 and 365 nm in solution as listed in Table 4. For example, Pt(chpe)(mnt) (**4a**) and Pt(chpe)(ecda) (**4b**) possess intense absorptions at 364 nm (27.5×10^3 cm^{-1}, 6100 M^{-1} cm^{-1}) and 350 nm (28.6×10^3 cm^{-1}, 31 000 M^{-1} cm^{-1}), respectively. In addition, all of the complexes containing monodentate phosphines, except $Pt(PMe_2Ph)_2$(ecda) (**8b**), have a broad shoulder into the visible region of the spectrum. The effect of changing from bidentate diphosphine to monodentate phosphines for a given Pt(dithiolate) is illustrated in Figure 4 for Pt(dppe)(mnt) (**1a**) and $Pt(PPh_3)_2$(mnt) (**7a**). The strong absorption bands exhibited by the Pt(diphosphine)(dithiolate) complexes are insensitive to changes in solvent polarity, in contrast with the intense solvatochromic absorptions seen in the 400–450-nm region of the spectra of Pt(diimine)(dithiolate) complexes. The λ_{max} of Pt(dppb)(ecda) (**3b**), for example, changes only from 346 nm (28.9×10^3 cm^{-1}) in $CHCl_3$ to 340 nm (29.4×10^3 cm^{-1}) in MeCN.

(32) The theoretical aspects of this argument are displayed in: Abraham, R. J.; Loftus, P. *Proton and Carbon-13 NMR Spectroscopy*; Heyden and Son, Ltd.: London, 1980; Chapter 4.
(33) Caruso, F.; Camalli, M.; Pellizer, G.; Asaro, F.; Lenarda, M. *Inorg. Chim. Acta* **1991**, *181*, 167.
(34) Mason, R.; Rae, A. I. M. *J. Chem. Soc. A* **1970**, 1767.
(35) Chan, L. T.; Chen. H.-W.; Fackler, J. P.; Masters, A. F.; Pan, W.-H. *Inorg. Chem.* **1982**, *21*, 4291.
(36) Weigand, W.; Bosl, G.; Polborn, K. *Chem. Ber.* **1990**, *123*, 1339.
(37) Cavell, K. J.; Jin, H.; Skelton, B. W.; White, A. H. *J. Chem. Soc., Dalton Trans.* **1992**, 2923.
(38) Günter, W.; Gliemann, G.; Klement, U.; Zabel, M. *Inorg. Chim. Acta* **1989**, *165*, 51.
(39) Welch, J. H.; Bereman, R.; Singh, P. *Inorg. Chim. Acta* **1989**, *163*, 93.
(40) Kobayashi, A.; Sasaki, Y. *Bull. Chem. Soc. Jpn.* **1977**, *50*, 2650.
(41) Coucouvanis, D.; Baenziger, N. C.; Johnson, S. M. *Inorg. Chem.* **1974**, *13*, 1191.
(42) Eisenberg, R.; Ibers, J. A. *Inorg. Chem.* **1965**, *4*, 605.
(43) Forrester, J. D.; Zalkin, A.; Templeton, D. H. *Inorg. Chem.* **1964**, *3*, 1507.

(a)

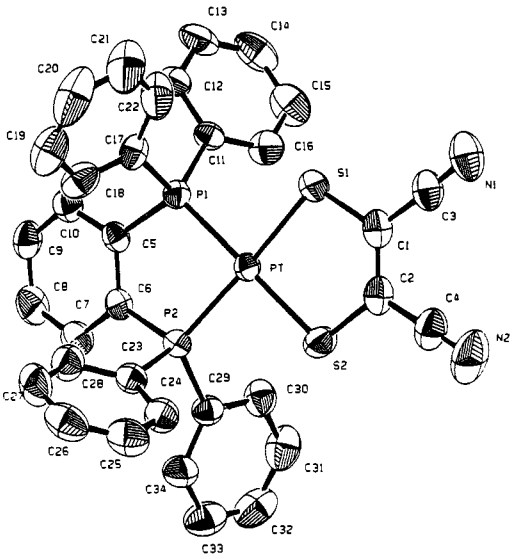

(b)

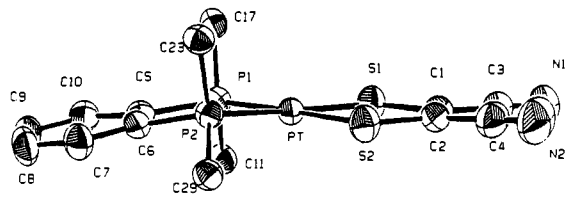

Figure 3. (a) Molecular structure and atom numbering of the non-hydrogen atoms (ORTEP diagram, 50% thermal ellipsoids) of Pt(dppb)(mnt) (**3a**). (b) Alternate view illustrating the 12.02° angle between the plane containing Pt, P, and S and that containing P, C5, C6, C7, C8, C9, and C10. The non-ipso phenyl carbons off of the phosphorus have been omitted for clarity.

Table 3. Selected Bond Distances (Å) and Angles (deg) for Pt(dppe)(mnt) (**1a**) and Pt(dppb)(mnt) (**3a**) with Atom Labels According to Figures 2 and 3, Respectively, and Estimated Standard Deviations in Parentheses

Pt(dppe)(mnt) (**1a**)		Pt(dppb)(mnt) (**3a**)	
	Distances		
Pt–S1	2.303(2)	Pt–S1	2.309(3)
Pt–S2	2.296(2)	Pt–S2	2.293(2)
Pt–P1	2.262(2)	Pt–P1	2.247(2)
Pt–P2	2.252(2)	Pt–P2	2.266(3)
P1–C5	1.840(8)	P1–C5	1.822(6)
P2–C6	1.823(8)	P2–C6	1.821(6)
C5–C6	1.54(1)	C5–C6	1.393(8)
S1–C1	1.727(7)	S1–C1	1.731(7)
S2–C2	1.737(7)	S2–C2	1.720(7)
C1–C2	1.34(1)	C1–C2	1.38(1)
C1–C3	1.43(1)	C1–C3	1.43(1)
C2–C4	1.42(1)	C2–C4	1.44(1)
	Angles		
S1–Pt–S2	89.46(7)	S1–Pt–S2	89.35(9)
P1–Pt–P2	85.65(7)	P1–Pt–P2	86.13(9)
Pt–S1–C1	101.8(3)	Pt–S1–C1	102.7(2)
Pt–S2–C2	102.5(2)	Pt–S2–C2	102.7(2)
Pt–P1–C5	108.3(2)	Pt–P1–C5	108.7(2)
Pt–P2–C6	105.7(2)	Pt–P2–C6	108.0(2)
S1–Pt–P2	172.42(7)	S1–Pt–P2	176.51(6)
S2–Pt–P1	174.54(7)	S2–Pt–P1	179.01(6)

Upon inspection of Table 4 one trend which seems evident is that ϵ_{max} for the intense absorption band is approximately five times higher in the ecda complexes than in the corresponding mnt derivatives. For Pt(dppv)(ecda) (**2b**), ϵ_{max}(340 nm, 29.4 × 10^3 cm^{-1}) is 33 560 M^{-1} cm^{-1}, while for Pt(dppv)(mnt) (**2a**), ϵ_{max}(356 nm, 28.1 × 10^3 cm^{-1}) is 6550 M^{-1} cm^{-1}. Another trend is that the absorption maximum is generally lower in energy in the mnt complexes than in the analogous ecda complexes. For example, λ_{max} is 356 nm (28.1 × 10^3 cm^{-1}) for Pt(dppe)(mnt) (**1a**) versus 344 nm (29.1 × 10^3 cm^{-1}) for Pt(dppe)(ecda) (**1b**).

Table 4. Room-Temperature Electronic Absorption Spectral Data[a]

complex no.	formula	λ, nm	λ, 10^3 cm^{-1}	ϵ_{max} (M^{-1} cm^{-1})
1a	Pt(dppe)(mnt)	356	28.1	6240
2a	Pt(dppv)(mnt)	356	28.1	6550
3a	Pt(dppb)(mnt)	358	27.9	6340
4a	Pt(chpe)(mnt)	364	27.5	6100
5a[b]	Pt(dppm)(mnt)	352	28.4	5950
7a[b]	$Pt(PPh_3)_2$(mnt)	366	27.3	6200
		410	24.3	515
8a	$Pt(PMe_2Ph)_2$(mnt)	353[c]	28.3	6110
10a[b]	$Pt(P(OPh)_3)_2$(mnt)	344[c]	29.1	5870
11a[b]	$Pt(P(OEt)_3)_2$(mnt)	353[c]	28.3	5260
1b	Pt(dppe)(ecda)	344	29.1	31330
2b	Pt(dppv)(ecda)	340	29.4	33560
3b	Pt(dppb)(ecda)	346	28.9	32570
4b	Pt(chpe)(ecda)	350	28.6	30985
5b	Pt(dppm)(ecda)	350	28.6	27430
6b	Pt(pompom)(ecda)	340	29.4	29600
7b	$Pt(PPh_3)_2$(ecda)	346[c]	28.9	27010
8b	$Pt(PMe_2Ph)_2$(ecda)	351	28.5	26890
9b	$Pt(PCy_3)_2$(ecda)	364	27.5	25490
		427	23.4	4910
10b	$Pt(P(OPh)_3)_2$(ecda)	340[c]	29.4	27840
11b	$Pt(P(OiPr)_3)_2$(ecda)-$(TBA)_2[Pt(mnt)_2]$[d]	340[c]	29.4	26950
		310	23.3	13400
		337	29.7	15600
		474	21.1	3470
		540	18.5	1220
		639	15.6	56
		694	14.4	49
	$(TBA)_2[Pt(i\text{-}mnt)_2]$[e]	312	32.0	18000
		352	28.4	3500
		413	24.2	55000

[a] Chloroform solutions. [b] Data taken from ref 16. [c] Broad tail into visible region. [d] Data taken from ref 45. [e] Data taken from ref 46.

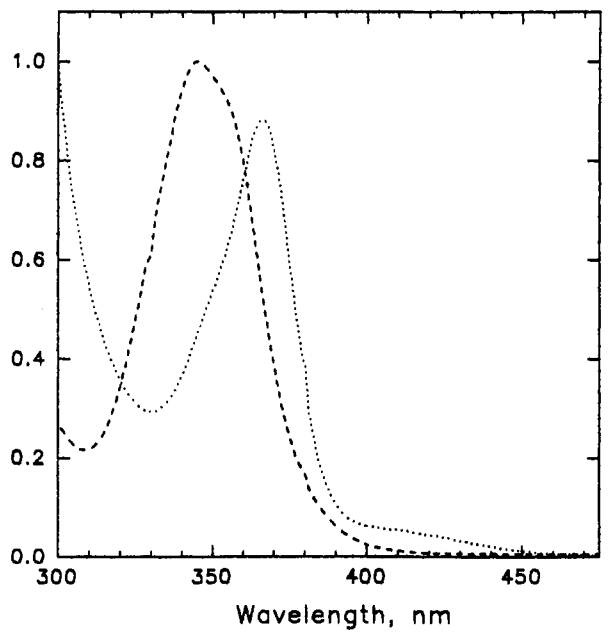

Figure 4. Room temperature electronic absorption spectrum in chloroform solution. Comparison of the effect of changing phosphine, (- - -) Pt(dppe)(mnt) (**1a**) and (···) $Pt(PPh_3)_2$(mnt) (**7a**).

Emission Spectroscopy. All of the complexes studied exhibit strong emission in rigid media at 77 K but only weak luminescence

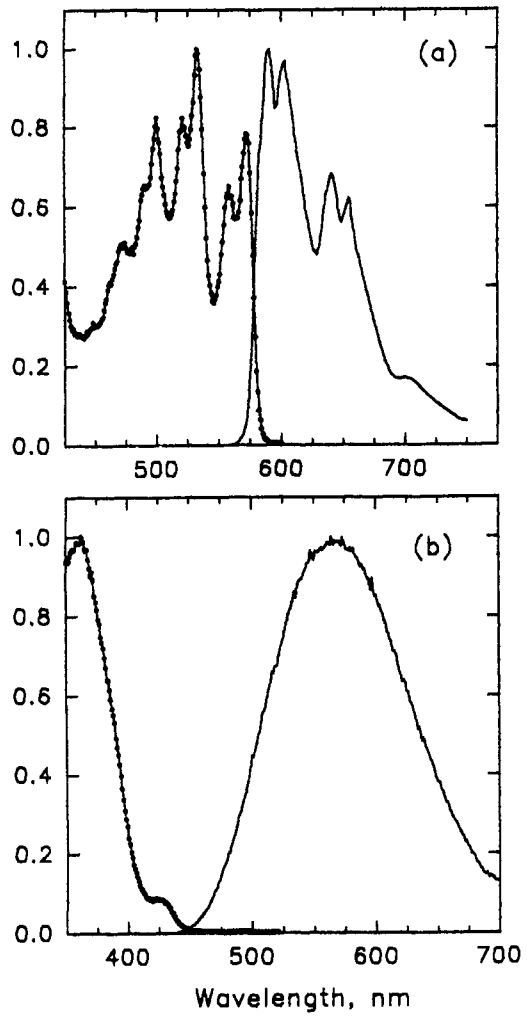

Figure 5. Low temperature emission (—, solid state, 77 K) and excitation (···, solid state, 77 K) of (a) Pt(dppb)(mnt) (**3a**) and (b) Pt(dppb)(ecda) (**3b**).

at room temperature in the solid state. In contrast with the Pt(diimine)(dithiolate) complexes, the diphosphine and bis(phosphine) dithiolate complexes described here do not show emission in fluid solution. Figure 5 illustrates the low-temperature emission and excitation spectra in KBr matrix for Pt(dppb)(mnt) (**3a**) and Pt(dppb)(ecda) (**3b**). The highest energy emission and lowest energy excitation maxima of the complexes are listed in Table 5. In KBr matrices and DMM glasses at 77 K, intense emission is observed that is independent of excitation wavelength. The emission in DMM glass is broader and blue-shifted compared to that in KBr matrix. In the mnt complexes, the emission spectrum shows rich vibrational structure with a large progression of 1375 cm^{-1} and a smaller spacing of 315 cm^{-1}, whereas for the ecda complexes the emission band is broad and featureless.

In general, the emission energy decreases with increasing donor ability of the phosphine ligand (Table 5) for the complexes containing monodentate phosphines. For example, the highest energy emission maximum decreases from 524 nm (19.1×10^3 cm^{-1}) for $Pt(P(OPh)_3)_2$(ecda) (**10b**), to 570 nm (17.5×10^3 cm^{-1}) for $Pt(PPh_3)_2$(ecda) (**7b**), to 574 nm (17.4×10^3 cm^{-1}) for $Pt(PCy_3)_2$(ecda) (**9b**) reflecting the increasing donor ability of the phosphine.[44] Also, the emission energy falls within two ranges dictated by the dithiolate present. The relative energy of λ_{em} for complexes **1–11** is much lower for the mnt complexes, falling between 566 and 621 nm ($(17.7–16.1) \times 10^3$ cm^{-1}), relative to that of the ecda complexes, which ranges from 510 to 570 nm ($(19.6–17.5) \times 10^3$ cm^{-1}) in a KBr matrix.

The excitation spectra show similar band shape differences between mnt and ecda complexes. The excitation spectra of the mnt complexes exhibit sharp, well-defined bands with a large progression of 1258 cm^{-1} and a smaller spacing of 492 cm^{-1}, whereas for the ecda complexes, the excitation spectra are featureless. The excitation maxima of all of the complexes extend to lower energies than bands observed in the respective absorption spectra of the complexes. Again, the lowest energy excitation maxima for complexes **1–11** fall within two distinct spectral regions dictated by the dithiolate. For the mnt complexes, the range is 542–585 nm ($(18.4–17.1) \times 10^3$ cm^{-1}). These complexes have a small apparent Stokes shift (100–1900 cm^{-1}). The ecda complexes, however, are different in that the lowest observed excitation maxima fall at much higher energies (416–427 nm, or $(24.0–23.4) \times 10^3$ cm^{-1}) than the highest emission maxima, yielding large apparent Stokes shifts (3900–6500 cm^{-1}).

Emission Lifetimes. Emission lifetimes in the solid state at 77 K are reported in Table 5. There is a marked difference between the samples containing mnt and ecda ligands. All of the mnt complexes exhibit single exponential decays with lifetimes on the order of 20–120 μs. In contrast, the ecda complexes show a complex decay that can be represented by the sum of two exponentials. In all cases, lifetimes for the ecda complexes are significantly shorter than those for the mnt analogues, ranging from 0.3 to 10 μs.

Assignment of the Emitting State. From the spectroscopic data described above and in Tables 4 and 5 and on the basis of previously reported assignments of transitions in related compounds.[5,16] it is possible to develop consistent assignments for the strongly allowed low energy absorption band and for the emissive excited state in the diphosphine and bis(phosphine) dithiolate complexes reported here. As noted above, all of the complexes possess strongly allowed absorption bands in the 340–365-nm region of the spectrum with molar extinction coefficients around 6000 and 30 000 M^{-1} cm^{-1} for mnt and ecda complexes, respectively. Similar transitions are seen for related 1,5-cyclooctadiene dithiolate complexes, (Pt(COD)(mnt) and Pt(COD)(ecda),[5] and analogous bands are observed in the spectra of the bis(dithiolate) dianions $Pt(mnt)_2^{2-}$ and $Pt(i\text{-}mnt)_2^{2-}$ where the ligand *i*-mnt has –CN in place of the –COOEt functionality of ecda.[45,46] Complexes prepared with ecda and *i*-mnt have optical properties that are virtually identical.[8] For Pt(COD)(mnt), the bands appear at 330 (30.3×10^3 cm^{-1}, ϵ_{max} = 7014 M^{-1} cm^{-1}) and 346 nm (28.9×10^3 cm^{-1}, ϵ_{max} = 6208 M^{-1} cm^{-1}), while for Pt(COD)(ecda), the analogous transitions occur at 340 (29.4×10^3 cm^{-1}, ϵ_{max} = 24 600 M^{-1} cm^{-1}) and 350 nm (28.6×10^3 cm^{-1}, ϵ_{max} = 25 300 M^{-1} cm^{-1}). These bands have previously been assigned as $d–\pi^*_{dithiolate}$ charge-transfer transitions. The corresponding electronic transitions of $Pt(mnt)_2^{2-}$ and $Pt(i\text{-}mnt)_2^{2-}$ occur at much lower energies. Specifically, for $Pt(mnt)_2^{2-}$, the metal-to-dithiolate charge-transfer transitions are observed at 474 (21.1×10^3 cm^{-1}, ϵ_{max} = 3470 M^{-1} cm^{-1}) and 540 nm (18.5×10^3 cm^{-1}, ϵ_{max} = 1220 M^{-1} cm^{-1}) while for $Pt(i\text{-}mnt)_2^{2-}$ the MLCT transition occurs at 413 nm (24.2×10^3 cm^{-1}, ϵ_{max} = 55 000 M^{-1} cm^{-1}). It is thus evident that the strongly allowed bands in the 340–365 nm region for the Pt(diphosphine)(dithiolate) complexes and related bis(phosphine) derivatives which are also seen in the COD dithiolate analogs and at lower energies in the bis(dithiolate) dianions correspond to metal-to-dithiolate charge-transfer transitions. The large discrepancy between molar extinction coefficients for the mnt and ecda systems relates to differences in the electronic structures of these dithiolates, and most particularly, in the $\pi^*_{dithiolate}$ orbitals of the 1,2- and 1,1-dithiolates.[11] The higher energy for the $d–\pi^*_{dithiolate}$ MLCT transitions in the neutral Pt dithiolate complexes relative to those in the $Pt(S–S)_2^{2-}$

(44) Crabtree, R. H. In *The Organometallic Chemistry of the Transition Metals*; Wiley-Interscience: New York, 1988; pp 71–74.

(45) Shupack, S. I.; Billig, E.; Clark, R. J. H.; Williams, R.; Gray, H. B. *J. Am. Chem. Soc.* **1964**, *86*, 4594.

(46) Werden, B. G.; Billig, E.; Gray, H. B. *Inorg. Chem.* **1966**, *5*, 10027.

Table 5. Electronic Emission and Excitation Spectral Data at 77 K in Solid KBr Matrix and in Rigid DMM[a] glass

complex		KBr matrix		DMM Matrix		
no.	formula	highest energy em max, nm[b]	lowest energy exc max, nm[b]	highest energy em max, nm[b]	lowest energy exc max, nm[b]	τ, μs
1a	Pt(dppe)(mnt)	621 (16.1)	568 (17.6)	589 (17.0)	566 (17.7)	76
2a	Pt(dppv)(mnt)	610 (16.4)	579 (17.3)			77
3a	Pt(dppb)(mnt)	590 (16.9)	573 (17.4)			119
4a	Pt(chpe)(mnt)	610 (16.4)	570 (17.5)			66
5a[c]	Pt(dppm)(mnt)	610 (16.4)	570 (17.5)			
7a[c]	$Pt(PPh_3)_2$(mnt)	652 (15.3)	585 (17.1)	597 (16.8)	570 (17.5)	24
8a	$Pt(PMe_2Ph)_2$(mnt)	584 (17.1)	572 (17.5)			
10a[c]	$Pt(POPh_3)_2$(mnt)	605 (16.5)	542 (18.4)			
11a[c]	$Pt(POEt_3)_2$(mnt)	566 (17.7)	560 (17.8)	579 (17.3)	553 (18.1)	
1b	Pt(dppe)(ecda)	540 (18.5)	425 (23.5)	490 (20.4)	422 (23.7)	0.36
2b	Pt(dppv)(ecda)	510 (19.6)	425 (23.5)	485 (20.6)	422 (23.7)	0.37, 9.0
3b	Pt(dppb)(ecda)	567 (17.6)	426 (23.5)	492 (20.3)	424 (23.6)	0.27, 0.46
4b	Pt(chpe)(ecda)	545 (18.3)	423 (23.6)	479 (20.9)	422 (23.7)	0.31, 4.23
5b	Pt(dppm)(ecda)	565 (17.7)	427 (23.4)	491 (20.4)	425 (23.5)	
6b	Pt(pompom)(ecda)			478 (20.9)	420 (23.8)	
7b	$Pt(PPh_3)_2$(ecda)	570 (17.5)	416 (24.0)	495 (20.2)	425 (23.5)	0.37, 10.1
8b	$Pt(PMe_2Ph)_2$(ecda)			489 (20.4)	427 (23.4)	
9b	$Pt(PCy_3)_2$(ecda)	574 (17.4)	426 (23.5)			
10b	$Pt(POPh_3)_2$(ecda)	524 (19.1)	423 (23.6)	474 (21.1)	425 (23.5)	
11b	$Pt(POiPr_3)_2$(ecda)	514 (19.4)	423 (23.6)	478 (20.9)	424 (23.6)	

[a] DMF/methylene chloride/methanol (1:1:1 v/v/v). [b] Values in parentheses are reported in wavenumbers, $\times 10^3$ cm^{-1}. [c] Data taken from ref 16.

complexes is consistent with lower d orbital energies in the neutral systems as compared with those in the dianionic complexes.

In addition to the strongly allowed metal–dithiolate MLCT absorptions, there are also shoulders that extend into the visible region of the spectrum with molar absorptivities in the range 500–7000 M^{-1} cm^{-1}. For example, ϵ_{max} is 4910 for $Pt(PCy_3)_2$(ecda) at 427 nm (23.4 $\times$ 10^3 cm^{-1}). The magnitude of the extinction coefficients for these shoulders tends to rule against a metal-centered d–d transition. A key point in considering the assignment of these shoulders is that irradiation into these bands at low temperature leads to observable emission. On the basis of this observation and the assignment of the strongly allowed transition given above, we assign these shoulders as the triplet state of the orbitally allowed metal-to-$\pi^*_{dithiolate}$ charge transfer.

The spectroscopic data described above for the Pt(diphosphine)(dithiolate) systems and the results of previously reported mnt and ecda complexes indicate that there are important and consistent differences between the emission spectra of mnt and ecda complexes. All of the mnt complexes including the diphosphine and bis(phosphine) systems described here, the COD[5] and diimine[8,9,11] derivatives reported previously, and the anionic Rh(I) and Ir(I) compounds of the type MLL'(mnt)$^-$, where L and L' are neutral 2e- donors,[16] show similar vibrational structures in both their emission and excitation spectra. The presence of this structure is thus independent of both metal and non-mnt ligands ranging from CO and diolefin to phosphines and diphosphines. The similarity of the emission and excitation spectra for all of the mnt complexes indicates that they possess a common emitting state which must involve the mnt ligand. In the emission spectra of these complexes, the resolved vibrational progression of $\sim$1375 cm^{-1} most closely corresponds to the C=C stretch of the mnt ligand.

A similar argument regarding emission band shape holds for the ecda analogues. All of the square planar ecda complexes including the diphosphine and bis(phosphine) systems reported here as well as Pt(COD)(ecda),[5] $Ir(CO)_2$(ecda)$^-$, and Ir(CO)(P(OPh)$_3$)(ecda)$^-$ [47] have featureless emission and excitation bands. The shape of the emission band is also independent of metal and non-ecda ligand. On the basis of the similar band shapes of the emission spectra among all of these ecda complexes, the emitting state involves the ecda ligand. The difference in appearance of the emission bands between the mnt and ecda complexes is undoubtedly related to the difference in the $\pi^*_{dithiolate}$ orbital and electronic structure of the two ligands.[11] Upon complexation, the mnt ligand forms a 5-membered chelate ring containing the C=C double bond that is coupled to the excited state, while ecda forms a 4-membered chelate ring with an exo C=C double bond.

Although the band shapes of the emission are different between the mnt and ecda complexes, the energy of the transition is affected similarly by changes in diphosphine chelate or bis(phosphine) ligands. Specifically, analysis of the data in Tables 4 and 5 shows that as the electron donor ability of the phosphine increases, the highest energy emission and lowest energy excitation and absorption maxima all decrease in energy. The trend of absorption and emission energy with phosphine ligand is rationalized in the following way. The energy of the metal d orbitals is influenced by the σ-donor and π-acceptor ability of the non-dithiolate ligands in a way such that as the overall electron donor ability of the ligands increases, the more electron rich the d^8 metal center becomes. This results in raising the energy of the essentially nonbonding and weakly antibonding metal d orbitals and leads to a red shift of the emission from a d–$\pi^*_{dithiolate}$ excited state. In the emissive state, the $\pi^*_{dithiolate}$ level is relatively unaffected by the overall electron donor ability of the non-dithiolate ligands, thereby explaining the observed λ_{em} dependence on L.

The possibility of a phosphine-involved excited state in complexes **1–11** is ruled out because the lowest unoccupied phosphine-centered orbitals are expected to be at much higher energy relative to the lowest unoccupied dithiolate orbital, $\pi^*_{dithiolate}$, and metal orbital, dσ^*. This is supported by a study of phosphorus chelates in M(P–P)$_2^+$ done by Fordyce and Crosby[2] who find that π orbitals on P are not strongly involved in charge transfer transitions within these complexes.

Also shown in Tables 4 and 5 is that the highest energy emission and lowest energy excitation and absorption maxima all occur at lower energy in the mnt complexes than in the ecda derivatives indicating that the π^* orbital of mnt is lower in energy than the corresponding orbital in ecda. This is most clearly illustrated for derivatives **1a** and **1b**, which have their first emission maxima at 621 (16.1 $\times$ 10^3 cm^{-1}) and 540 nm (18.5 $\times$ 10^3 cm^{-1}), their first excitation maxima at 568 (17.6 $\times$ 10^3 cm^{-1}) and 425 nm (23.5 $\times$ 10^3 cm^{-1}), and their absorption maxima at 356 (28.1 $\times$ 10^3 cm^{-1}) and 344 (29.1 $\times$ 10^3 cm^{-1}), respectively.

A molecular orbital study of Pt(diimine)(dithiolate) complexes supports the view that the π^*_{mnt} orbital lies lower in energy relative to the π^*_{ecda} (or $\pi^*_{i\text{-}mnt}$) orbital.[11] These extended Hückel

(47) Cummings, S. D.; Eisenberg, R. Unpublished results.

molecular orbital calculations show that the lowest unoccupied π^* dithiolate levels lie below the metal $d\sigma^*$ orbital of these square planar complexes and that the π^*_{mnt} level lies lower in energy than the π^* orbital of the 1,1-dithiolate *i*-mnt for a given (Pt(diimine) moiety.[11,48] For complexes **1–11** relative to the platinum(II) diimine dithiolate systems studied previously,[7-11] the absence of a $\pi^*_{diimine}$ level results in the absence of a solvatochromic charge-transfer band of interligand character and supports the assignment of the lowest energy emissive state in the present systems as being a $d-\pi^*_{dithiolate}$ charge transfer.

Although spin selection rules may be considerably relaxed due to spin–orbit coupling in third row transition-metal complexes,[49] evidence exists for substantial spin-forbidden character in the emission from these complexes. The excitation spectra of all of the complexes extend to lower energies than bands observed in the absorption spectra, consistent with the lowest energy excitations arising from transitions that are spin forbidden. Also, the relatively long emission lifetimes, ranging from 1 to 120 μs at 77 K, indicate that there is substantial spin-forbidden character in their emissive state. On the basis of these results, the emissive state in all of the Pt(II) diphosphine and bis(phosphine) dithiolates is assigned as $^3\{d-\pi^*_{dithiolate}\}$.

The observation of a biexponential decay lifetime in the ecda complexes may indicate the presence of two or more excited states, but more extensive temperature-dependent studies of emission quantum yields and lifetimes are required. Multiple state emission is not uncommon and has been observed in related complexes including those studied by Gliemann *et al.*,[50,51] Barigelletti *et al.*,[52] Zuleta *et al.*,[10] Glazen and Lees,[53] and Kirchoff *et al.*[54]

Conclusions

Pt(diphosphine)(dithiolate) complexes and related bis(phosphine) derivatives were synthesized to examine their emission behavior and to probe the effect of the dithiolate on their luminescence. The $^{31}P\{^1H\}$ NMR spectra of the mnt complexes show a single resonance, while the ecda complexes contain two doublets. The $^{31}P\{^1H\}$ NMR spectra of all of the complexes show platinum satellites ($^1J_{Pt-P}$ = 1100–2500 Hz) and all of the ecda complexes show complex second-order effects in their $^{31}P\{^1H\}$ spectrum owing to slight differences in J_{Pt-P} and similar chemical shifts for the inequivalent ^{31}P nuclei. The structures of two mnt complexes were established by single-crystal X-ray structure determinations to be square planar with minor deviations from the idealized geometry. The phosphine backbone of the chelate ring of Pt(dppb)(mnt) (**3a**) is nonplanar, deviating 12.02° from the plane containing the metal, phosphorus, and sulfur atoms. The complexes possess square planar coordination geometries with metrical parameters of the dithiolate chelate rings giving evidence of delocalization. All complexes are emissive in the solid state and in rigid media at low temperature and the shape of their emission bands is different depending on whether the dithiolate is mnt (1,2-dithiolate) or ecda (1,1-dithiolate). On the basis of the emission results including lifetimes and by comparison with other emissive dithiolate complexes, the emissive state is assigned as $^3\{d-\pi^*_{dithiolate}\}$.

Acknowledgment. We wish to thank the Department of Energy, Division of Chemical Sciences, and Eastman Kodak Co., Inc. for support of this research. A generous loan of platinum salts from Johnson Matthey Aesar/Alfa Co. is also gratefully acknowledged.

Supplementary Material Available: Complete listing of crystallographic details, bond lengths and bond angles, positional, and anisotropic thermal parameters for **1a** and **3a** (17 pages). Ordering information is given on any current masthead page.

(48) The ligand *i*-mnt has –CN in place of the –COOEt functionality of ecda and was used for computational simplicity.

(49) Crosby, G. A.; Hipps, K. W.; Elfring, W. H. *J. Am. Chem. Soc.* **1974**, *96*, 629.
(50) Biedermann, J.; Gliemann, G.; Klement, U.; Range, K.-J.; Zabel, M.; *Inorg. Chim. Acta* **1990**, *171*, 35.
(51) Schlattl, K.; Gliemann, G.; Jolliet, P.; von Zelewsky, A. *Chem. Phys. Lett.* **1990**, *168*, 505.
(52) For example, Barigelletti, F.; Sandrini, D.; Maestri, M.; Balzani, V.; von Zelewsky, A.; Chassot, L.; Jolliet, P.; Maeder, U. *Inorg. Chem.* **1988**, *27*, 3644 and references therein.
(53) Glazen, M. M.; Lees, A. J. *J. Am. Chem. Soc.* **1989**, *111*, 6602.
(54) Kirchoff, J. R.; Gamache, D. R.; Blaskie, M. W.; Del Paggio, A. A.; Lengel, R. K.; McMillin, D. R. *Inorg. Chem.* **1983**, *22*, 2380.